ORIGINAL ARTICLE

WILEY

Imaging-based risk stratification of patients with pulmonary embolism based on dual-energy CT-derived radiomics

Jennifer Gotta[1] | Vitali Koch[1] | Tobias Geyer[1] | Simon S. Martin[1] | Christian Booz[1] | Scherwin Mahmoudi[1] | Katrin Eichler[1] | Philipp Reschke[1] | Tommaso D'Angelo[2] | Konrad Klimek[3] | Thomas J. Vogl[1] | Leon D. Gruenewald[1]

[1]Goethe University Hospital Frankfurt, Frankfurt am Main, Germany

[2]Department of Biomedical Sciences and Morphological and Functional Imaging, University of Messina, Messina, Italy

[3]Goethe University Frankfurt, University Hospital, Clinic for Nuclear Medicine, Frankfurt am Main, Germany

Correspondence
Jennifer Gotta, University Hospital Frankfurt, Theodor-Stern-Kai 7, 60590 Frankfurt am Main, Germany.
Email: jennifergotta@aol.com

Abstract

Background: Technological progress in the acquisition of medical images and the extraction of underlying quantitative imaging data has introduced exciting prospects for the diagnostic assessment of a wide range of conditions. This study aims to investigate the diagnostic utility of a machine learning classifier based on dual-energy computed tomography (DECT) radiomics for classifying pulmonary embolism (PE) severity and assessing the risk for early death.

Methods: Patients who underwent CT pulmonary angiogram (CTPA) between January 2015 and March 2022 were considered for inclusion in this study. Based on DECT imaging, 107 radiomic features were extracted for each patient using standardized image processing. After dividing the dataset into training and test sets, stepwise feature reduction based on reproducibility, variable importance and correlation analyses were performed to select the most relevant features; these were used to train and validate the gradient-boosted tree models.

Results: The trained machine learning classifier achieved a classification accuracy of .90 for identifying high-risk PE patients with an area under the receiver operating characteristic curve of .59. This CT-based radiomics signature showed good diagnostic accuracy for risk stratification in individuals presenting with central PE, particularly within higher risk groups.

Conclusion: Models utilizing DECT-derived radiomics features can accurately stratify patients with pulmonary embolism into established clinical risk scores. This approach holds the potential to enhance patient management and optimize patient flow by assisting in the clinical decision-making process. It also offers the advantage of saving time and resources by leveraging existing imaging to eliminate the necessity for manual clinical scoring.

1 | INTRODUCTION

Pulmonary embolism (PE) is the third leading cause of death from cardiovascular disease following myocardial infarction and stroke.[1–3] Despite advances in diagnostic techniques and treatment options, PE remains a significant cause of morbidity and mortality both within hospitals and outside of them.[1,2] Timely diagnosis and accurate risk stratification are critical for optimal treatment and the prevention of further complications such as chronic thromboembolic pulmonary hypertension and recurrent thromboembolic events. Computed tomography pulmonary angiography (CTPA) remains the gold standard for the diagnosis of PE with sensitivity and specificity close to 100%.[4,5]

The incorporation of machine learning (ML) into diverse medical fields is gaining significant prominence. This development has the potential to reduce the workload of healthcare professionals and accelerate the diagnostic process, ultimately culminating in more efficient and effective patient care.[6–8]

Technically, ML refers to the development of algorithms and models that enable computers to learn from experience without being explicitly programmed. In comparison to general Artificial Intelligence (AI), ML is a subset that focuses on machine learning through data analysis. Concerning interpretability and the ability for human guidance, ML models, particularly deep neural networks, frequently present a challenge known as the 'black-box' problem. This implies that comprehending the decision-making processes of these models can be intricate.[9,10]

Furthermore, there has been growing interest in the application of radiomics – a quantitative methodology to extract visually not assessable texture features from medical imaging.[11,12] This rapidly advancing field has ushered in a new era of diagnostic possibilities with the potential to revolutionize medical imaging and clinical decision-making. The integration of spectral information obtainable in dual-energy computed tomography (DECT) with radiomics holds great promise in redefining how we understand and manage PE.

Therefore, this study aimed to explore the potential of DECT-derived radiomics for advanced risk stratification in patients with pulmonary embolism. Through this integrated approach, we hope to bridge the gap from clot to clarity, offering a novel perspective on risk assessment in pulmonary embolism and paving the way for more precise and tailored patient care.

2 | METHODS

This retrospective study was approved by the local Ethical Committee (University Hospital Frankfurt am Main, 2021-498_1), which waived the requirement to obtain written informed consent. All analyses were conducted in accordance with local data protection regulations.

2.1 | Study population

Consecutive patients who underwent CT pulmonary angiogram (CTPA) for the detection or exclusion of PE between January 2015 and March 2022 were considered for inclusion in this study. Eligible examinations were identified from the picture archiving and communication system (Centricity™ Version 7.0 General Electric Healthcare). Inclusion criteria were patients over 18 years with a confirmed PE and the presence of a dedicated CTPA examination depicting the complete lung vasculature. Exclusion criteria were imaging artefacts in the pulmonary artery region, inadequate visual delineation of the embolus, incomplete examination of the pulmonary vasculature and insufficient clinical data. The selection process of the study participants is illustrated in Figure 1.

2.2 | Clinical and laboratory data acquisition

Electronic patient files and patient questionnaires were used to extract patient data and clinical parameters, including laboratory data, medical history, medication and hospital stays, the level of inpatient care and complications. For all patients, Wells Score and Pulmonary Embolism Severity Index (PESI) were calculated and classified into risk classes based on PESI (ranging from 1 to 5) and current ESC guidelines (low-risk PE, intermediate low-risk PE, intermediate high-risk PE and high-risk PE).[13]

FIGURE 1 Flowchart of patient inclusion. PE, pulmonary embolism.
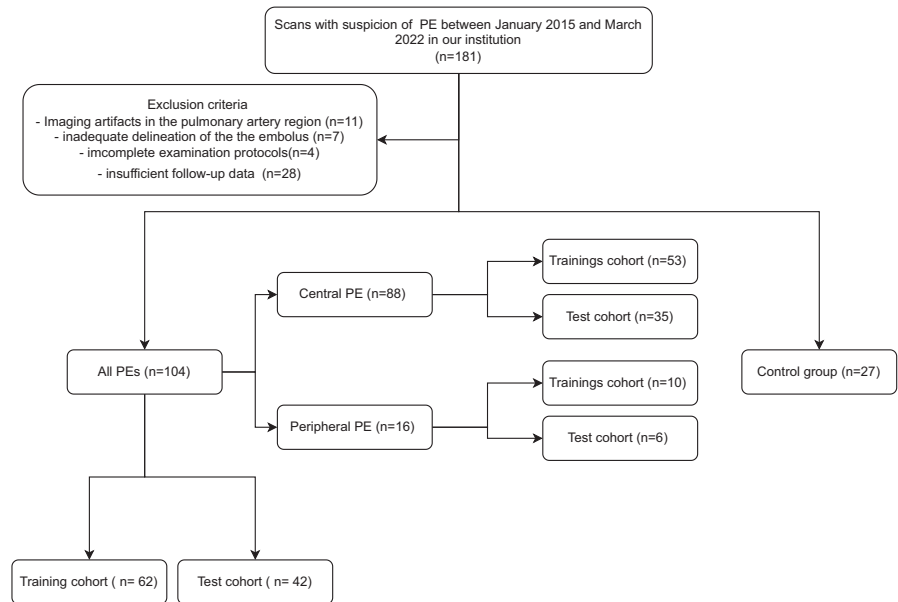
2.3 | Image acquisition and evaluation

CT examinations were performed on a third-generation dual-source dual-energy CT (Somatom Force, Siemens Healthineers) with the following acquisition parameters: tube A, 90 kVp, 190 mAs; tube B, Sn150 kVp; .25 s rotation time, 1–2 s acquisition time, 192 × .6 mm collimation, 2.5 pitch value. Scanning was performed in the craniocaudal direction in bolus-triggered arterial and venous phases with 80–120 mL of nonionized contrast agent (Imeron 400 MCT mg Iod/mL, Bracco) at an injection rate of 5–6 mL/s, a threshold of 120 HU and a delay of 7 s. Image evaluation was performed by a separate readout of two board-certified radiologists (L.D.G and V.K), blinded to clinical data and previous imaging results. All patients were classified into three different groups (1 = central PE, 2 = peripheral PE, 3 = no PE). In case of disagreement, a third reader (S.M) with 4 years of experience was consulted. Reported is the majority decision.

2.4 | Image segmentation and analysis

CT datasets from all patients were anonymized, extracted as Digital Imaging and Communications in Medicine (DICOM) datasets, and uploaded into proprietary software (3D Slicer version 5.0.2, Harvard University). Manual measurement was used to obtain the diameters of the pulmonary trunk (mm), right ventricle (RV, mm), left ventricle (LV, mm) and the RV/LV quotient. A separate segmentation of the embolus and the pulmonary trunk including both pulmonary arteries was performed in each patient using the interactive segmentation algorithm GrowCut.[14–16] The data of the control group were

utilized for the segmentation process. An example of the final segmentation of the embolus and pulmonary artery is shown in Figure 2. All segmentations were independently evaluated for anatomic accuracy by two experienced radiologists (C.B. and S.S.M). In case of disagreement with the initial result by either radiologist, the segmentation process was repeated until considered appropriate. All radiologists involved in the evaluation were blinded towards patient data, including clinical data and imaging reports.

2.5 | Extraction of radiomics features

Radiomic feature extraction was performed using the PyRadiomics extension package for 3D Slicer (Version 5.1.0–2022-05–20) and yielded a total of 107 features per segmentation[17] (Table S1). All extracted features were categorized as described below: Grey-Level Dependence Matrix (GLDM), Grey-Level Co-Occurrence Matrix (GLCM), Grey-Level Run Length Matrix (GLRLM), Grey-Level Size Zone Matrix (GLSZM), Neighboring Grey Tone Difference Matrix (NGTDM), Shape and First Order.[17] The radiomics quality score based on the Checklist for the valuation of Radiomics Research (CLEAR) is given in the Figure S1.[18]

2.6 | Radiomics feature selection

Feature selection was conducted using a multi-step feature selection procedure. After applying Z-score standardization to normalize all numeric features, the Boruta dimension reduction and feature elimination algorithm
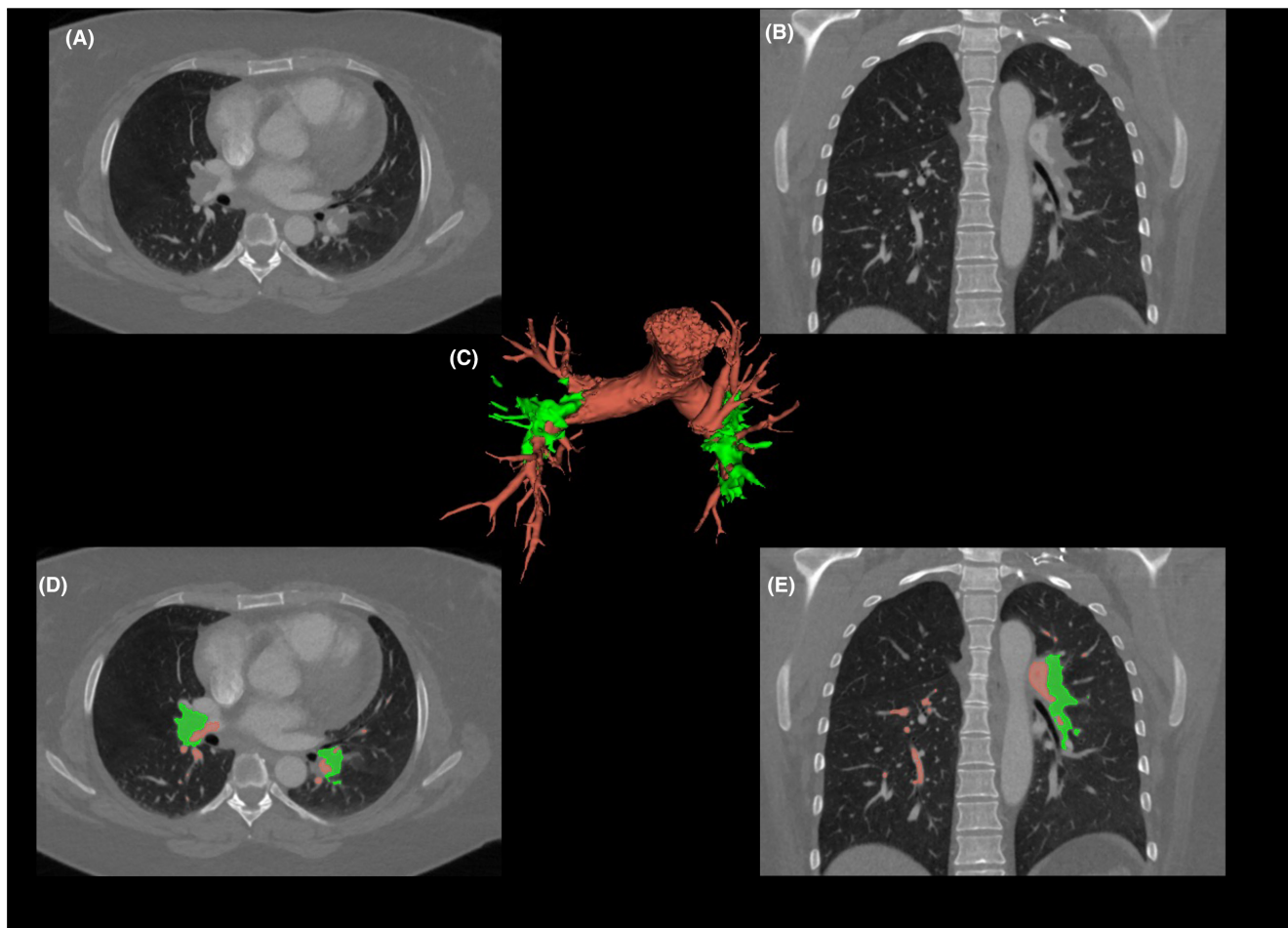
FIGURE 2 Exemplary segmentation of the pulmonary embolus and pulmonary artery. Embolic material in the pulmonary arteries is illustrated in green, and contrast agent in the pulmonary artery is illustrated in red. (A) unsegmented axial slice; (B) unsegmented coronal slice; (C) final segmentation of the embolus and pulmonary artery; (D) segmented axial slice; (E) segmented coronal slice. PE, pulmonary embolism.

was applied as previously described.[19,20] Furthermore, a correlation matrix was conducted to identify clusters of highly correlated features, defined by Pearson's $r \geq .60$ to reduce the features. The most important features were finally selected based on their Gini index (Table S2).

2.7 | Construction of the radiomics model

A gradient-boosted tree model was trained on the most important radiomic features to classify patients with central PE into the four different risk categories (low-risk PE, intermediate low-risk PE, intermediate high-risk PE and high-risk PE) using a training dataset comprising 53 patients. The model was then evaluated on a separate test dataset containing 35 patients, which was not used during training of the algorithm.

A second gradient-boosted tree model was trained to classify the patients with peripheral PE in an identical approach. Another gradient-boosted tree model with all patients with PE was also trained.

2.8 | Statistical analysis

Statistical analysis was performed using R statistical software (R Foundation for Statistical Computing; Version 2023.06.0+421) and MedCalc (MedCalc Software Ltd.; Version 20.123). Gaussian distribution of the data was assessed using the Wilk–Shapiro test. Normally distributed values were expressed as mean$\pm$SD and non-normally distributed values were represented as median and interquartile range (IQR). The t-test was employed for data with a continuous distribution, whereas the Mann–Whitney test or Spearman rank correlation coefficient was applied to non-normally distributed data.

Receiver operating characteristic (ROC) curve analysis was used to obtain diagnostic accuracy parameters. A p-value$< .05$ was considered statistically significant.

TABLE 1 Baseline characteristics of the study population.

Variables n (%) or mean (SD)	Central PE (n = 88)	Peripheral PE (n = 16)	No PE (n = 27)	p-value
Demographics				
Overall age (years)	61 ± 15	67 ± 13	63 ± 17	.294
Male sex (n)	53 (60%)	7 (43.8%)	16 (59%)	
Female sex (n)	35 (40%)	9 (56.2%)	11 (41%)	
Vital signs				
Heart rate (bpm)	100 ± 25	83 ± 23	–	**.0095**
Respiratory rate (/min)	21 ± 8	18 ± 6	–	.2237
Systolic blood pressure (mmHg)	133 ± 32	141 ± 26	–	.4343
Diastolic blood pressure (mmHg)	78 ± 17	78 ± 12	–	.9284
Saturation of peripheral oxygen (SpO2, %)	92 ± 5	91 ± 6	–	.6607
Temperature (°C)	36.9 ± 0.4	37 ± 1	–	.9428
Echocardiographic findings				
TAPSE (mm)	19.15 ± 5.15	24 ± 6	–	**.0112**
sysPAP (mmHg)	49.15 ± 16.57	42.7 ± 12.1	–	.3637
Laboratory parameters				
D-dimers (ng/mL)	15,547 ± 1895	5527 ± 3947		**<.0001**
Troponin T (pg/mL)	90 ± 116	44.65 ± 48.96		**.0381**
NT-proBNP (pg/mL)	5298 ± 8226	1802.63 ± 2500.64		**.0337**
CT measurements				
Truncus pulmonalis diameter (mm)	30.5 ± 3.7	26.63 ± 3.28	–	**.0006**
RV diameter (mm)	44.03 ± 7.7	39.36 ± 9.53	–	**.0333**
LV diameter (mm)	31.33 ± 8.0	38.16 ± 6.92	–	**.0015**
RV/LV ratio	1.49 ± 0.45	1.06 ± 0.31	–	**.0004**
Clinical scores				
Wells-score	6 ± 2	4.0 ± 2.1	–	**.0020**
PESI-score	102 ± 41	101.4 ± 30.5	–	.7163
Low-risk group	5 (6%)	4 (25%)		
Intermediate low-risk group	18 (20%)	7 (44%)		
Intermediate high-risk group	57 (65%)	5 (32%)		
High-risk group	8 (9%)	0 (0%)		
Risk factors				
Oral contraceptive (n)	3 (3%)	0 (0%)	–	
Chemotherapy within the last 4 weeks (n)	7 (7%)	1 (6.3%)	–	
Obesity (n)	33 (38%)	4 (25%)	–	
Immobilization within the last 4 weeks	41 (48%)	6 (37.5%)	–	
Surgery within the last 4 weeks (n)	17 (18%)	3 (18.8%)	–	
Thrombophilia (n)	13 (15%)	2 (12.5%)	–	
Atrial fibrillation (n)	13 (13%)	0 (0%)	–	
Cancer (n)	25 (28%)	6 (37.5%)	–	
Diabetes mellitus (n)	15 (17%)	2 (12.5%)	–	
Arterial hypertension (n)	37 (42%)	7 (43.8%)	–	
Current smoking (n)	10 (11%)	3 (18.8%)	–	
Inflammatory bowel disease (n)	2 (2%)	0 (0%)	–	

(Continues)

TABLE 1 (Continued)

Variables n (%) or mean (SD)	Central PE (n = 88)	Peripheral PE (n = 16)	No PE (n = 27)	p-value
Coronary heart disease (n)	4 (5%)	1 (6.3%)	–	
Initial treatment				
Lysis (n)	10 (11%)	0 (0%)	–	
Lysis in course (n)	6 (7%)	0 (0%)	–	
Unfractionated heparin (n)	57 (65%)	4 (25%)	–	
Low-molecular weight heparin (n)	23 (26%)	10 (62.5%)	–	
Oral anticoagulants (n)	7 (8%)	3 (18.8%)	–	
Hospital stay				
Length of hospital stay from event (days)	11 ± 7	8.4 ± 5.9	–	.2605
Complications (n)	21 (24%)	3 (18.8%)	–	
Recurrence PE (n)	3 (3%)	1 (6.3%)	–	
Death caused by PE (n)	2 (2%)	0 (0%)	–	

Abbreviations: LV, left ventricle; NT-proBNP, N-terminal prohormone of brain natriuretic peptide; PE, pulmonary embolism; PESI, Pulmonary Embolism Severity Index; RV, right ventricle; sysPAP, systolic pulmonary artery pressure; TAPSE, tricuspid annular plane systolic excursion. Significance is presented in bold.

3 | RESULTS

3.1 | Patient characteristics

A total of 181 patients were considered for study inclusion. Exclusion criteria were imaging artefacts in the pulmonary artery region ($n=11$), inadequate visual delineation of the embolus ($n=7$), incomplete examination protocols ($n=4$) and insufficient follow-up data ($n=28$). Thus, the final study population consisted of 131 patients (55 female, 76 male, mean age $64±15$ years). Eighty-eight patients (67%) were diagnosed with central pulmonary embolism (PE) and 16 patients (12%) were diagnosed with peripheral PE. Twenty-seven patients without PE served as the control group.

No significant differences were observed concerning the patient's gender in both cohorts ($p=.425$) as well as concerning the age (mean age 61 and 67 years for central and peripheral PE, respectively, $p=.294$). Detailed socio-demographic and clinical characteristics are given in Table 1.

3.2 | Clinical risk stratification

In the central pulmonary embolism (PE) group, the majority of patients (65%) were classified as intermediate high risk. Conversely, in the peripheral PE group, most patients (44%) were categorized as intermediate low risk. Wells Scores were higher in the group of patients with central PE ($p=.002$), but no significant differences were observed for PESI ($p=.7163$).

Heart rate ($p<.001$), D-dimers ($p<.0001$) and CT-derived metrics such as RV/LV-ratio ($p<.0004$) and truncus pulmonalis diameter ($p<.0006$) showed significant differences between patients with central and peripheral PE.

3.3 | Selected radiomics features for predicting risk classes

The radiomics feature extraction yielded a total of 107 features per segmentation (Table S1). After feature reduction, 12 features remained in the central PE group, 7 features remained in the peripheral PE group and 15 features remained in the group with all PEs. The correlation matrices for all features are given in Figure 3. The features ultimately included based on the Gini index are given in Table 2.

3.4 | Radiomics model performance for predicting risk classes

Based on the training dataset, the final model achieved the highest classification accuracy when classifying patients into the high-risk category within the central test cohort, achieving an accuracy of .91.

Table 3 provides a comprehensive overview of the classification accuracy, sensitivity, specificity and AUC.

In the central test cohort, it achieved an AUC of .86 (95% CI, .645–.856; Youden index in relation to the radiomics features, .38) in the high-risk class and in the peripheral test cohort an AUC of .63 (95% CI, .38–.869, Youden-Index, .0012) in the intermediate high-risk class. Details are given in Figure 4.
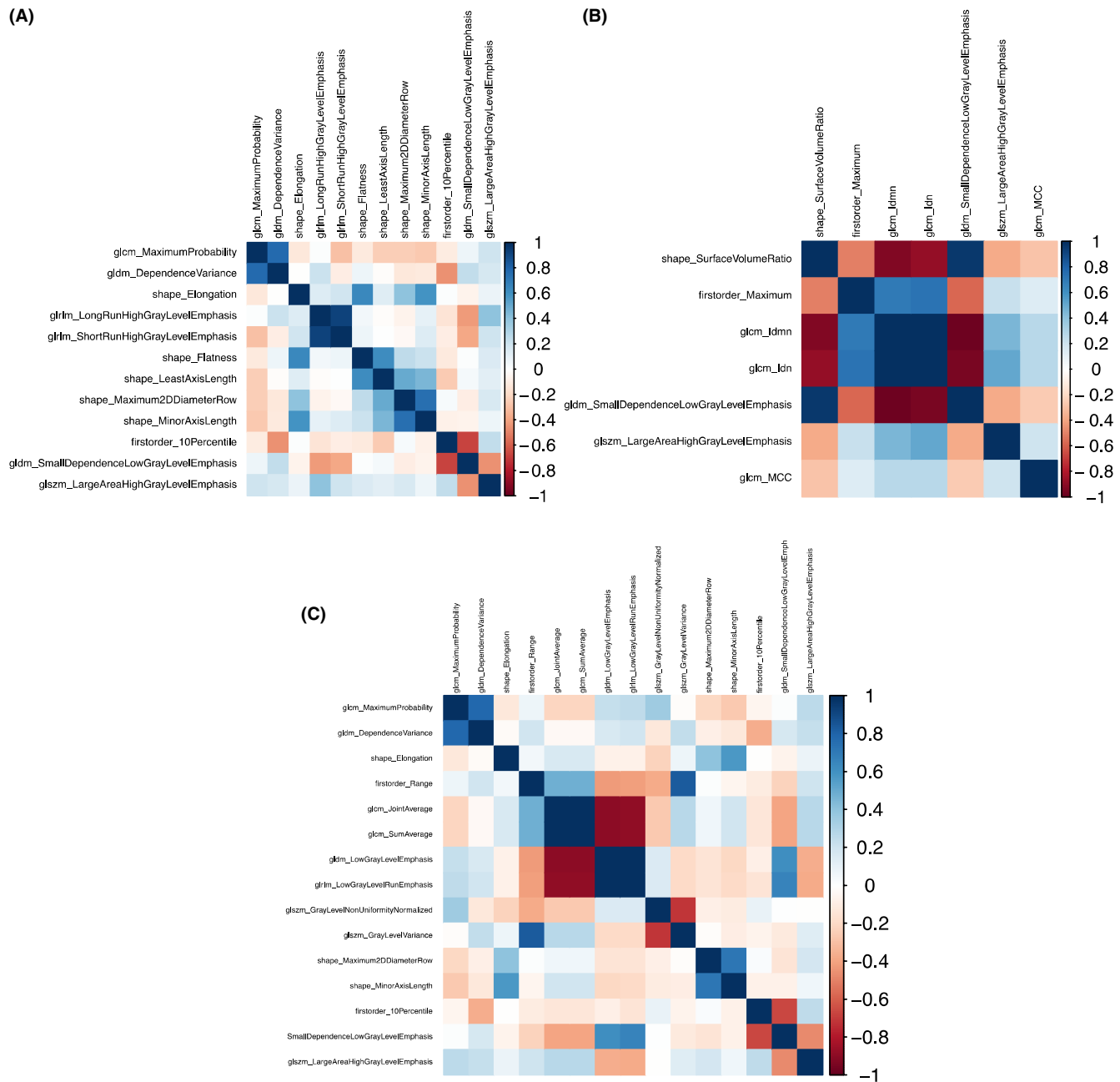
FIGURE 3 Correlation matrices. Correlation matrices of the most important features. (A) central PE group; (B) peripheral PE group; (C) all PEs. GLCM, Grey-Level Co-Occurrence Matrix; GLDM, Grey-Level Dependence Matrix; GLRLM, Grey-Level Run Length Matrix; GLSZM, Grey-Level Size Zone Matrix; MCC, maximal correlation coefficient; NGTDM, Neighboring Grey Tone Difference Matrix; PE, pulmonary embolism.

3.5 | Agreement between the radiomics model and the clinical risk score

The inter-reader agreement between the clinical risk stratification based on the ESC score[13] and the radiomics model classification demonstrated a strong concordance between the radiomics model and the clinical risk score, as indicated by a weighted kappa of .984 (95% CI .953–1.0).

4 | DISCUSSION

Pulmonary embolism (PE) remains a significant cause of morbidity and mortality both within hospitals and outside of them. To guide patient management, accurate and timely risk stratification based on various underlying clinical factors is essential. Here, we demonstrate that the integration of spectral imaging with a radiomics-based machine learning classifier can perform an accurate risk

TABLE 2 The most important radiomics features.

Features	Central PE	Peripheral PE	All PE
	gldm_DependenceVariance	shape_SurfaceVolumeRatio	gldm_DependenceVariance
	shape_Elongation	firstorder_Maximum	shape_Elongation
	glrlm_ShortRunHighGrayLevelEmphasis	glszm_LargeAreaHighGrayLevelEmphasis	firstorder_Range
	shape_MinorAxisLength	glcm_ maximal correlation coefficient (MCC)	glcm_SumAverage
	firstorder_10Percentile		gldm_SmallDependenceLowGrayLevelEmphasis
	gldm_SmallDependenceLowGrayLevelEmphasis		glszm_GrayLevelNonUniformityNormalized
			firstorder_10Percentile
			glszm_LargeAreaHighGrayLevelEmphasis

Abbreviations: LV, left ventricle; NT-proBNP, N-terminal prohormone of brain natriuretic peptide; PE, pulmonary embolism; PESI, Pulmonary Embolism Severity Index; RV, right ventricle; sysPAP, systolic pulmonary artery pressure; TAPSE, tricuspid annular plane systolic excursion.

stratification of patients with PE based on established clinical guidelines with a diagnostic accuracy of 90%.[13,21]

Our findings from the central PE group in both the training and test cohorts demonstrated an accuracy of 100% and 91%, respectively, in classifying high-risk PE cases. These results highlight the model's effectiveness, particularly in accurately identifying patients with high-risk PE. The stronger performance in classifying high-risk cases suggests that our model could serve as a tool in clinical decision-making for high-risk PE patients, enabling timely interventions and optimized management strategies for those at greater risk of adverse outcomes. This is underlined by the agreement between clinically obtained risk scores and model performance.

In contrast, our model for the peripheral PE group did not yield satisfactory results, primarily attributed to the restricted number of patients within this cohort. Nonetheless, the model exhibited good results proficiency, particularly in its ability to accurately identify patients at a high risk of PE. Consequently, further studies with larger patient cohorts are warranted to improve the model's performance. The limited sample size in the peripheral PE group may have hindered the model's ability to achieve significant predictive accuracy.

The dataset for peripheral PE was insufficient due to a lack of patients in this cohort due to our strict exclusion criteria, primarily attributed to an inadequate delineation of the thrombus and incomplete imaging of the pulmonary vasculature due to radiation concerns in some patients. Therefore, conducting studies with a more extensive and diverse patient population would be essential to enhance the reliability and generalizability of the model's findings. By expanding the dataset, we can better capture the heterogeneity of PE cases in both cohorts and develop a more robust and reliable predictive model for this specific group of patients.

Several clinical-radiological scores have been developed to assess the risk of patients with PE for early (in-hospital or 30 day) death. Of these, the ESC score has been shown to perform best with an sensitivity of around 95%.[13,21–25] To our knowledge, the reported approach represents the first attempt to apply radiomics to DECT images for the classification of patients with acute PE into dedicated risk types. Integrating our classifier into routine clinical practice holds the potential for substantial time and resource savings. By leveraging existing DECT imaging, the need for manual clinical scoring could be eliminated to streamline patient management and accelerate and optimize clinical decision making. An exemplary workflow might involve the well-established execution of CTPA in the initial step. Subsequently, automated segmentation is performed and the determination of the risk group is carried out using an advanced model for risk assessment.

TABLE 3 Performance of the radiomics model.

	Central PE group	Peripheral PE group	All PE
AUC			
Low-risk PE	.62	.75	.60
Intermediate low-risk PE	.67	.5	.60
Intermediate high-risk PE	.69	.63	.63
High-risk PE	.86	–	.59
Sensitivity			
Low-risk PE	.00	1.0	.5
Intermediate low-risk PE	.45	1.0	.15
Intermediate high-risk PE	.88	1.0	.98
High-risk PE	.00	–	.17
Specificity			
Low-risk PE	.84	1.0	.75
Intermediate low-risk PE	.86	–	.98
Intermediate high-risk PE	.50	–	.43
High-risk PE	1.00	–	.96
Accuracy			
Low-risk PE	.77	.33	.77
Intermediate low-risk PE	.77	.33	.77
Intermediate high-risk PE	.74	–	.74
High-risk PE	.91	–	.90
PPV			
Low-risk PE	.00	1.0	.12
Intermediate low-risk PE	.45	.33	.67
Intermediate high-risk PE	.74	–	.75
High-risk PE	–	–	.34
NPV			
Low-risk PE	.94	1.0	.96
Intermediate low-risk PE	.86	–	.82
Intermediate high-risk PE	.71	.66	.90
High-risk PE	.90	–	.92

Note: The radiomics model's performance on the test datasets in classifying patients with acute PE in the four different risk categories (low-risk PE, intermediate low-risk PE, intermediate high-risk PE and high-risk PE).

Abbreviations: AUC, area under the curve; NPV, negative predictive value; PE, pulmonary embolism; PPV, positive predictive value.

However, the incorporation of automated segmentations in DECT images is imperative for seamless integration into clinical practice.[26] Therefore, further advancements in automated segmentation are required to facilitate seamless integration into clinical practice.

Early-risk assessment is crucial for the adequate management of patients with acute PE. The identification of high-risk patients enables timely interventions and optimized treatment strategies to minimize complications and to improve the patient's outcome. Previous studies showed that a delayed diagnosis of PE leads to a more unfavourable prognosis compared to an early diagnosis.[27] Additionally, PEs and their subsequent complications pose a substantial burden on healthcare systems and economies worldwide.[28]

Our study has several limitations that warrant consideration. First, this study was retrospectively conducted at a single centre. While this decision was intentionally taken in order to reduce potential differences related to scanners and scanner protocols that may arise from various manufacturers or different generations of scanners, the expansion of our study population is required to ensure generalizability of our results.

In the peripheral PE group, the limited number of patients posed a challenge, restricting the statistical power for this subgroup analysis. Finally, we did not include
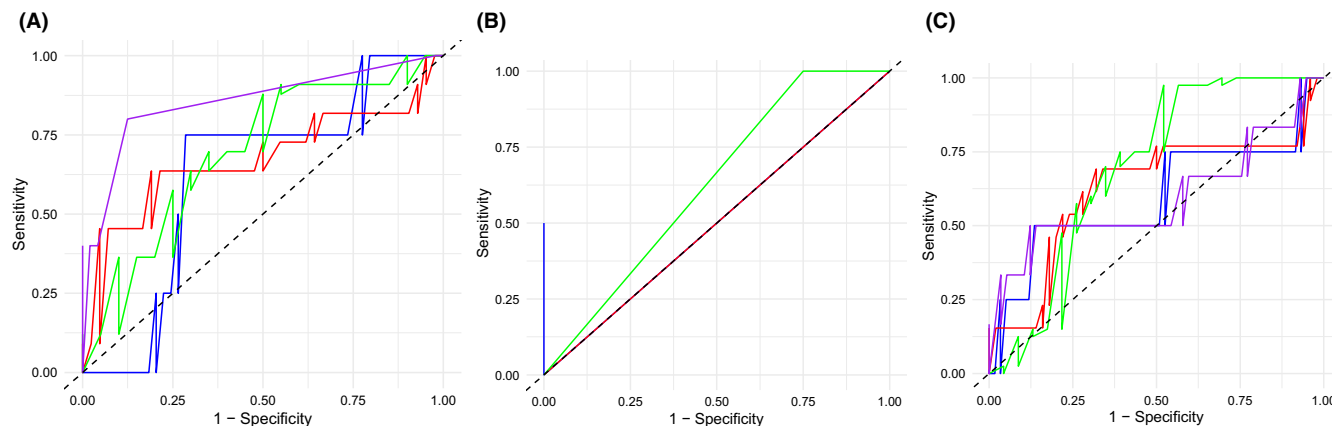
FIGURE 4 ROC analysis. The ROC analysis indicates sensitivity, and specificity of the gradient-boosted tree trained on the selected most important radiomic features. Blue, low-risk PE; red, intermediate low-risk; green, intermediate high-risk; purple, high risk. (A) central PE group; (B) peripheral PE; (C) all PEs. PE, pulmonary embolism; ROC, receiver operating characteristic.

clinical variables into our radiomics approach, although this might have led to a further increase in diagnostic performance. However, we aimed to focus on a purely radiomics-based model for classifying patients with acute PE into the four risk types, omitting the incorporation of clinical variables. While this approach aimed to explore the potential of radiomics alone, future studies could explore the integration of clinical variables to potentially enhance diagnostic performance.

Additionally, our model yielded the most promising outcomes when classifying the high-risk patient group. However, it is important to acknowledge that patients experiencing hemodynamic instability, classified as high risk, are easiest to identify using the clinical risk scores recommended by the ESC guidelines.

Finally, there is a lack of patient follow-up to validate the accuracy of risk classification using both clinical evaluation and radiomics approaches. In conclusion, our study demonstrates the promising potential of applying radiomics on DECT imaging to classify patients with acute PE into four distinct risk types. This novel approach holds the potential to improve clinical decision-making and patient management in the context of acute PE. By accurately stratifying patients into different risk categories, our radiomics-based classifier can potentially save valuable time and resources, as it leverages existing DECT imaging, eliminating the need for an additional scoring system. Further validation and integration of this approach with existing clinical tools could lead to improved outcomes and optimized patient care, ultimately advancing risk assessment and management for patients with acute PE.

AUTHOR CONTRIBUTIONS

All authors have contributed significantly to this work, participating in the conception, design, analysis, interpretation of data and writing/editing of this manuscript. J.G. and LD.G wrote the manuscript and designed the research. The other authors were involved in the analysis of the data and performed research. All authors revised the manuscript.

CONFLICT OF INTEREST STATEMENT

C.B. received speaking fees from Siemens Healthineers. The other authors have no potential conflict of interest to disclose.

DATA AVAILABILITY STATEMENT

All data and information used are included in this manuscript.

STATISTICS AND BIOMETRY

No complex statistical methods were necessary for this paper.

ORCID

Jennifer Gotta https://orcid.org/0000-0002-0524-6574
Vitali Koch https://orcid.org/0000-0001-6915-5906
Tommaso D'Angelo https://orcid.org/0000-0003-0004-6378

REFERENCES

1. Goldhaber SZ, Bounameaux H. Pulmonary embolism and deep vein thrombosis. *The Lancet.* 2012;379(9828):1835-1846. doi:10.1016/S0140-6736(11)61904-1

2. Sung YK, Kline JA. Unchanging mortality from pulmonary embolism in the United States. *Annals ATS*. 2023;20(11):1554-1556. doi:10.1513/AnnalsATS.202308-751ED

3. Zghouzi M, Mwansa H, Shore S, et al. Sex, racial, and geographic disparities in pulmonary embolism-related mortality Nationwide. *Ann Am Thorac Soc*. 2023;20(11):1571-1577. doi:10.1513/AnnalsATS.202302-091OC

4. Patel P, Patel P, Bhatt M, et al. Systematic review and meta-analysis of test accuracy for the diagnosis of suspected pulmonary embolism. *Blood Adv*. 2020;4(18):4296-4311. doi:10.1182/bloodadvances.2019001052

5. Monti CB, Zanardo M, Cozzi A, et al. Dual-energy CT performance in acute pulmonary embolism: a meta-analysis. *Eur Radiol*. 2021;31(8):6248-6258. doi:10.1007/s00330-020-07633-8

6. Xi L, Kang H, Deng M, et al. A machine learning model for diagnosing acute pulmonary embolism and comparison with Wells score, revised Geneva score, and years algorithm. *Chinese Med J*. 2023. 10.1097,ISS 0366-6999, 2542-5641. doi:10.1097/CM9.0000000000002837

7. Than MP, Pickering JW, Sandoval Y, et al. Machine learning to predict the likelihood of acute myocardial infarction. *Circulation*. 2019;140(11):899-909. doi:10.1161/CIRCULATIONAHA.119.041980

8. Islam NU, Zhou Z, Gehlot S, Gotway MB, Liang J. Seeking an optimal approach for computer-aided diagnosis of pulmonary embolism. *Med Image Anal*. 2023;91:102988. doi:10.1016/j.media.2023.102988

9. Rubinger L, Gazendam A, Ekhtiari S, Bhandari M. Machine learning and artificial intelligence in research and healthcare. *Injury*. 2023;54(Suppl 3):S69-S73. doi:10.1016/j.injury.2022.01.046

10. Ramkumar PN, Kunze KN, Haeberle HS, et al. Clinical and research medical applications of artificial intelligence. *Art Ther*. 2021;37(5):1694-1697. doi:10.1016/j.arthro.2020.08.009

11. Mayerhoefer ME, Materka A, Langs G, et al. Introduction to radiomics. *J Nucl Med*. 2020;61(4):488-495. doi:10.2967/jnumed.118.222893

12. Kocak B, Baessler B, Cuocolo R, Mercaldo N, Pinto Dos Santos D. Trends and statistics of artificial intelligence and radiomics research in radiology, nuclear medicine, and medical imaging: bibliometric analysis. *Eur Radiol*. 2023;33(11):7542-7555. doi:10.1007/s00330-023-09772-0

13. Konstantinides SV, Meyer G, Becattini C, et al. 2019 ESC guidelines for the diagnosis and management of acute pulmonary embolism developed in collaboration with the European Respiratory Society (ERS). *Eur Heart J*. 2020;41(4):543-603. doi:10.1093/eurheartj/ehz405

14. Velazquez ER, Parmar C, Jermoumi M, et al. Volumetric CT-based segmentation of NSCLC using 3D-slicer. *Sci Rep*. 2013;3(1):3529. doi:10.1038/srep03529

15. Egger J, Kapur T, Fedorov A, et al. GBM volumetry using the 3D slicer medical image computing platform. *Sci Rep*. 2013;3(1):1364. doi:10.1038/srep01364

16. Gonzalo Domínguez M, Hernández C, Ruisoto P, Juanes JA, Prats A, Hernández T. Morphological and volumetric assessment of cerebral ventricular system with 3D slicer software. *J Med Syst*. 2016;40(7):154. doi:10.1007/s10916-016-0510-9

17. Fedorov A, Beichel R, Kalpathy-Cramer J, et al. 3D slicer as an image computing platform for the quantitative imaging network. *Magn Reson Imaging*. 2012;30(9):1323-1341. doi:10.1016/j.mri.2012.05.001

18. Kocak B, Baessler B, Bakas S, et al. CheckList for EvaluAtion of radiomics research (CLEAR): a step-by-step reporting guideline for authors and reviewers endorsed by ESR and EuSoMII. *Insights Imaging*. 2023;14(1):75. doi:10.1186/s13244-023-01415-8

19. Kursa MB, Rudnicki WR. Feature selection with the Boruta package. *J Stat Soft*. 2010;36(11):1-3. doi:10.18637/jss.v036.i11

20. Degenhardt F, Seifert S, Szymczak S. Evaluation of variable selection methods for random forests and omics data sets. *Brief Bioinform*. 2019;20(2):492-503. doi:10.1093/bib/bbx124

21. Surov A, Thormann M, Bär C, Wienke A, Borggrefe J. Validation of clinical-radiological scores for prognosis of mortality in acute pulmonary embolism. *Respir Res*. 2023;24(1):195. doi:10.1186/s12931-023-02489-0

22. Surov A, Akritidou M, Bach AG, et al. A new index for the prediction of 30-day mortality in patients with pulmonary embolism: the pulmonary embolism mortality score (PEMS). *Angiology*. 2021;72(8):787-793. doi:10.1177/0003319721993346

23. Bova C, Sanchez O, Prandoni P, et al. Identification of intermediate-risk patients with acute symptomatic pulmonary embolism. *Eur Respir J*. 2014;44(3):694-703. doi:10.1183/09031936.00006114

24. Kumamaru KK, Saboo SS, Aghayev A, et al. CT pulmonary angiography-based scoring system to predict the prognosis of acute pulmonary embolism. *J Cardiovasc Comput Tomogr*. 2016;10(6):473-479. doi:10.1016/j.jcct.2016.08.007

25. Solverson K, Humphreys C, Liang Z, et al. Rapid prediction of adverse outcomes for acute normotensive pulmonary embolism: derivation of the Calgary acute pulmonary embolism score. *ERJ Open Research*. 2021;7(2):00879-2020. doi:10.1183/23120541.00879-2020

26. Woznicki P, Laqua F, Bley T, Baeßler B. AutoRadiomics: a framework for reproducible radiomics research. *Front Radiol*. 2022;2:919133. doi:10.3389/fradi.2022.919133

27. Mansella G, Keil C, Nickel CH, et al. Delayed diagnosis in pulmonary embolism: frequency, patient characteristics, and outcome. *Respiration*. 2020;99(7):589-597. doi:10.1159/000508396

28. Beckman MG, Hooper WC, Critchley SE, Ortel TL. Venous thromboembolism: a public health concern. *Am J Prev Med*. 2010;38:S495-S501. doi:10.1016/j.amepre.2009.12.017

SUPPORTING INFORMATION

Additional supporting information can be found online in the Supporting Information section at the end of this article.